

Quantum metastability in time-periodic potentials

Chung-Chieh Lee

Department of Electronic Engineering, Tung Nan Institute of Technology, Shengkeng, Taipei 222, Taiwan

Choon-Lin Ho

Department of Physics, Tamkang University, Tamsui 25137, Taiwan

(Dated: Mar 30, 2005)

In this paper we investigate quantum metastability of a particle trapped in between an infinite wall and a square barrier, with either a time-periodically oscillating barrier (Model A) or bottom of the well (Model B). Based on the Floquet theory, we derive in each case an equation which determines the stability of the metastable system. We study the influence on the stability of two Floquet states when their Floquet energies (real part) encounter a direct or an avoided crossing at resonance. The effect of the amplitude of oscillation on the nature of crossing of Floquet energies is also discussed. It is found that by adiabatically changing the frequency and amplitude of the oscillation field, one can manipulate the stability of states in the well. By means of a discrete transform, the two models are shown to have exactly the same Floquet energy spectrum at the same oscillating amplitude and frequency. The equivalence of the models is also demonstrated by means of the principle of gauge invariance.

PACS numbers: 03.65.Xp, 33.80.Be, 74.50.+r

I. INTRODUCTION

Recent developments in powerful lasers have induced great theoretical and experimental interests in quantum systems under the influence of periodic driving fields. For example, an active topic in the field of atomic physics is the dynamical stabilization of atoms by intense high-frequency laser fields [1, 2, 3, 4]. Scattering of particles by a time-periodic potential is frequently used as a model for the photon-assisted tunneling and other quantum transport problems [5, 6, 7, 8, 9]. The interesting phenomena of coherent destruction of tunneling in a periodically driven two-level systems has also been discussed extensively in the last decade [10, 11].

Although diverse phenomena related to time-periodic potentials have been widely investigated, in our opinion the interesting issue of quantum decay through tunneling of a metastable system trapped in a time-dependent potential should receive more attention than it has thus far. Metastable systems which decay through tunneling exist and are of interest in many areas of studies, the most famous of which being the α -decay of atoms. In many realistic situations of decay processes, the metastable systems have to be treated as being influenced by time-dependent potentials. For example, in some versions of the inflationary models of the early universe [12], inflation is governed by a Higgs field trapped in a metastable state. Inflation ends when the metastable state decays to the true ground state of the universe. During inflation the universe expands exponentially. It is thus obvious that the metastable state of the Higgs field is trapped in a rapidly varying potential. Unfortunately, in these inflationary models the true forms of the time-dependent potentials are determined by the dynamics of the system itself. This inherent difficulty makes the complete analysis of time-dependent decay of the Higgs field rather difficult. It is therefore desirable to gain some insights first by studying metastability in various types of time-dependent potentials in simple quantum-mechanical models.

In our previous work [13] we have proposed a simple metastable system with a moving potential which has height and width scaled in a specific way introduced by Berry and Klein [14]. In that model we found that a small but finite nondecay probability could persist at large time limit for an expanding potential. Another class of time-dependent metastable system had been discussed by Fisher [15], in which he considered a generic class of static metastable well subjected to a weak time-periodic force. As the strength of the time-periodic force was taken to be small, it could be treated as a small time-dependent perturbation term. Fisher modified the standard (time-independent) WKBJ approach to include a weak time-dependent perturbation. He found that the weak time-periodic force always enhances the time average of the decay rate of the system. The potential considered by Fisher has a number of oscillator-like levels near its minimum. The opposite situation where only two levels are present was considered by Sokolovski [16], who studied the effect of a small AC field mixing two levels in the well on the tunneling rate in a semiclassical framework.

Recently, we have considered the problem of how the metastability of a quantum system used to model the α -decay was influenced by an oscillating barrier [17]. The Floquet formalism was adopted in our analysis, so that the periodic field needs not be treated perturbatively, and the number of states in the potential is not restricted. Our results show that an oscillating potential barrier generally makes a metastable system decay faster. However, the existence

of avoided crossings of metastable states can switch a less stable state to a more stable one, and vice versa. It is also found that increasing the amplitude of the oscillating field may change a direct crossing of states into an avoided one. Hence, by a combination of adiabatic changes of the frequency and the amplitude of the oscillating barrier, one can manipulate the stability of different states in a quantum potential. If in the static well there exists a bound state, then it is possible to stabilize a metastable state by adiabatically changing the oscillating frequency and amplitude of the barrier so that the unstable state eventually crosses over to the stable bound state. In this connection we note here that a related problem was studied in [18], where the authors consider trapping an electron in thermal equilibrium within an infinite wall and a barrier which grows in time. There the confinement of particle in the well is achieved through the increase in the barrier height, whereas in our case it is accomplished mainly through the tuning up of the frequency of the oscillating barrier.

In [17] our main concern was the effect of avoided crossing on the quantum metastability in a periodically oscillating potential. In this paper we shall present a detailed study of the effect of direct crossing on the stability of a metastable system, and of how the oscillating amplitude affects the nature of direct/avoided crossings. We consider a simple quantum system in which a particle is trapped in between an infinite wall and a rectangular barrier. Two versions of the system are discussed. In Model A we consider the potential with an oscillatory height, while in Model B we make the bottom of the well oscillate instead. As in our previous work, the Floquet approach is adopted here. In each model, an equation which relates the Floquet quasienergy of the driven system to the amplitude and frequency of the time-periodic potential is obtained. This equation is solved numerically and the stability of the system is investigated as the frequency and amplitude of the oscillating field vary. To our surprise, the two models, very different in nature, turn out to possess the same Floquet energy spectrum (and thus the same stability). A discrete transform connecting the two models is found which explains the exactness of the Floquet spectrum. A physical understanding of the equivalence of the two models is also given based on the principle of gauge invariance.

The organization of the paper is as follows. In Sect. II, we will first briefly describe a simple metastable model of α -decay. Sect. III then introduces a modified model to include a time-periodically oscillating barrier (Model A). We will also describe the Floquet theory which we adopt in our analysis. The effects of the time-periodically oscillating barrier on the quantum metastability of the system is studied numerically in Sect. IV. Model B, which has the bottom of the well oscillating, is described in Sect. V. Sect. VI and Sect. VII present, respectively, the discrete transform and the gauge transformation that connect the two models. Sect. VIII summarizes the paper.

II. SIMPLE STATIC MODEL OF QUANTUM METASTABLE SYSTEM

A simple one-dimensional model to describe the phenomena of α -decay is that of a particle trapped in between an infinite potential wall and a finite barrier [19]. The barrier potential of such a metastable system can be expressed as

$$V(x) = \begin{cases} \infty, & x < 0, \\ V_0 > 0, & a \leq x \leq b, \\ 0, & 0 \leq x < a, \text{ and } x > b. \end{cases} \quad (1)$$

The wave function of the system has the well-known form $\Psi(x, t) = \psi(x)exp(-iEt/\hbar)$, where $\psi(x)$ satisfies the time-independent Schrödinger equation,

$$\left[-\frac{\hbar^2}{2m} \frac{d^2}{dx^2} + V(x) \right] \psi(x) = E\psi(x). \quad (2)$$

The wave function can be expressed in each regions as

$$\psi(x) = \begin{cases} A \sin(kx) + B \cos(kx), & 0 \leq x < a, \quad k = \sqrt{2mE/\hbar^2}, \\ C e^{qx} + D e^{-qx}, & a \leq x \leq b, \quad q = \sqrt{2m(V_0 - E)/\hbar^2}, \\ F e^{ikx} + G e^{-ikx}, & b < x. \end{cases} \quad (3)$$

Besides the ordinary boundary conditions which require that the wave function and its first derivative be continuous at the boundaries $x = a$ and b , we could also impose another two boundary conditions on the wave function by physical consideration. One is $B = 0$ as the wave function must vanish at the origin ($x = 0$); the other is $G = 0$ since there is no extra nonvanishing potential in the region $x > b$ to reflect wave from the right-hand side of the barrier. This later condition was first introduced by Gamow [20], Curney and Condon [21], and is usually called the ‘‘Gamow’s outgoing wave boundary condition’’ in the literature. With these boundary conditions, we can eliminate the remaining

coefficients (A, C, D, F) of the wave function and obtain an equation that determines the eigenenergy of the system,

$$\frac{q}{k} \tan ka + 1 = \frac{q + ik}{q - ik} \left(\frac{q}{k} \tan ka - 1 \right) e^{-2q(b-a)}. \quad (4)$$

By solving the above equation numerically for a given barrier height V_0 , one finds that the solution of Eq.(4) gives complex eigenenergy, $E = E_0 - i\Gamma/2$. The imaginary part is related to the decay rate of the state. Despite some conceptual difficulties concerning the nature of complex energy, this simple approach by imposing Gamow's outgoing wave boundary condition successfully describes the exponential decay of metastable systems [19, 22].

III. MODEL A: THE STATIC MODEL WITH A TIME-PERIODICALLY OSCILLATING BARRIER

We now modify the static model to include a time-periodically oscillating barrier,

$$V(x, t) = \begin{cases} \infty, & x < 0, \\ V_0 + V_1 \cos(\omega t), & a \leq x \leq b, \\ 0, & 0 \leq x < a, \text{ and } x > b, \end{cases} \quad (5)$$

where $V_0 > 0$ and $0 < V_1 < V_0$. Unlike the static case, in this time-dependent model we have to solve the time-dependent Schrödinger equation,

$$i\hbar \frac{\partial \Psi(x, t)}{\partial t} = \left[-\frac{\hbar^2}{2m} \frac{\partial^2}{\partial x^2} + V(x, t) \right] \Psi(x, t). \quad (6)$$

A similar time-periodically oscillating potential (without the infinite wall) has been used to investigate electrons scattering in a time-dependent potential by Li and Reichl [8]. They employed the Floquet formalism to set up the S-matrix of the driven system. The advantage of the Floquet formalism is that one could do away with any restriction of the amplitude and frequency of the driving force. Here we will mainly follow the procedure developed in [8] to construct the wave function of our model of metastable system.

The Floquet theorem states that the wave function of a time-periodic system has the form $\Psi_\varepsilon(x, t) = e^{-i\varepsilon t/\hbar} \Phi_\varepsilon(x, t)$, where $\Phi_\varepsilon(x, t)$ is a periodic function $\Phi_\varepsilon(x, t) = \Phi_\varepsilon(x, t+T)$ with the period $T = 2\pi/\omega$, and ε is the Floquet quasienergy, or simply the Floquet energy. It should be noted that the Floquet energy is determined only modulo $\hbar\omega$. For if $\{\varepsilon, \Phi_\varepsilon\}$ is a solution of the Schrödinger equation, then $\{\varepsilon' = \varepsilon + n\hbar\omega, \Phi_{\varepsilon'} = \Phi_\varepsilon \exp(in\omega t)\}$ is also a solution for any integer n . But they are physically equivalent as the total wave function Ψ_ε is the same [23]. All physically inequivalent states can be characterized by their reduced Floquet energies in a zone with a width $\hbar\omega$. We therefore consider solutions of ε only in the first Floquet zone, i.e. $\varepsilon \in [0, \hbar\omega)$.

The Schrödinger equation inside the region of the oscillating barrier $a \leq x \leq b$ is

$$-i\hbar \frac{\partial}{\partial t} \Phi_\varepsilon(x, t) - \frac{\hbar^2}{2m} \frac{\partial^2}{\partial x^2} \Phi_\varepsilon(x, t) + [V_0 + V_1 \cos(\omega t)] \Phi_\varepsilon(x, t) = \varepsilon \Phi_\varepsilon(x, t). \quad (7)$$

Letting $\Phi_\varepsilon(x, t) = g(x)f(t)$, Eq.(7) can be separated into

$$-\frac{\hbar^2}{2m} \frac{d^2 g(x)}{dx^2} + V_0 g(x) = E g(x), \quad (8)$$

and

$$i\hbar \frac{df(t)}{dt} - V_1 \cos(\omega t) f(t) = (E - \varepsilon) f(t), \quad (9)$$

where E is a constant to be determined from the periodicity of the function $f(t)$, i.e. $f(t+T) = f(t)$. Eq.(9) can be integrated to give

$$f(t) = e^{-i(E-\varepsilon)t/\hbar} e^{-iV_1 \sin(\omega t)/\hbar\omega}, \quad (10)$$

where we have set the initial condition as $f(0) = 1$. The second factor in Eq.(10) can be rewritten using the identity [24]

$$e^{-iV_1 \sin(\omega t)/\hbar\omega} = \sum_{n=-\infty}^{\infty} J_n(\alpha) e^{-in\omega t} \quad ; \quad \alpha = \frac{V_1}{\hbar\omega}, \quad (11)$$

where $J_n(\alpha)$ is the Bessel function of the first kind. Eq.(10) then reduces to

$$f(t) = e^{-i(E-\varepsilon)t/\hbar} \sum_{n=-\infty}^{\infty} J_n(\alpha) e^{-in\omega t} . \quad (12)$$

The periodic condition $f(t+T) = f(t)$, which reads

$$f(t+T) = e^{-i(E-\varepsilon)(t+T)/\hbar} \sum_{n=-\infty}^{\infty} J_n(\alpha) e^{-in\omega(t+T)} , \quad (13)$$

$$= e^{-i(E-\varepsilon)t/\hbar} \sum_{n=-\infty}^{\infty} J_n(\alpha) e^{-in\omega t} e^{-i(E-\varepsilon+n\hbar\omega)T/\hbar} , \quad (14)$$

$$= f(t) , \quad (15)$$

requires that $(E - \varepsilon + n\hbar\omega)T/\hbar = 2m\pi$ ($m = \text{integer}$). So the constant E can only assume the following values

$$E_l = \varepsilon + l\hbar\omega , \quad l = m - n = \text{integer} . \quad (16)$$

The allowed values of E indicate that the time-periodic potential will generate side-band structures with $E_l = \varepsilon + l\hbar\omega$ as the ‘‘side-band energy’’ of the l -th side-band.

Knowing the allowed values of the constant E_l , we can now solve Eq.(8) to get

$$g(x) = \sum_l a_l e^{q_l x} + b_l e^{-q_l x} , \quad q_l = \sqrt{2m(V_0 - \varepsilon - l\hbar\omega)/\hbar^2} . \quad (17)$$

Combining Eq.(12) and Eq.(17), we obtain the wave function inside the region of the oscillating barrier $a \leq x \leq b$,

$$\begin{aligned} \Psi_{II}(x, t) &= e^{-i\varepsilon t/\hbar} \sum_n \sum_l (a_l e^{q_l x} + b_l e^{-q_l x}) J_{n-l}(\alpha) e^{-in\omega t} , \\ &\equiv \sum_n \sum_l (a_l e^{q_l x} + b_l e^{-q_l x}) J_{n-l}(\alpha) e^{-iE_n t/\hbar} . \end{aligned} \quad (18)$$

Having gotten the wave function inside the region $a \leq x \leq b$, the continuity of the wave function and its first derivative at the boundaries $x = a$ and b at any time requires that outside the region $a \leq x \leq b$ there are nonvanishing wave functions on each side-band channel. Therefore the wave function in the region $0 \leq x < a$ is

$$\Psi_I(x, t) = \sum_n A_n \sin(k_n x) e^{-iE_n t/\hbar} , \quad k_n = \sqrt{2mE_n/\hbar^2} , \quad (19)$$

which vanishes at the origin, $\Psi_I(0, t) = 0$. On the other hand, the Gamow’s outgoing wave boundary condition suggests that the wave function in the region $x > b$ to have the form

$$\Psi_{III}(x, t) = \sum_n t_n e^{ik_n x} e^{-iE_n t/\hbar} . \quad (20)$$

We can obtain relations among the coefficients A_n, a_n, b_n and t_n by matching the boundary conditions at $x = a$ and b for each side-band. The results are

$$A_n \sin(k_n a) = \sum_l (a_l e^{q_l a} + b_l e^{-q_l a}) J_{n-l}(\alpha) , \quad (21)$$

$$k_n A_n \cos(k_n a) = \sum_l q_l (a_l e^{q_l a} - b_l e^{-q_l a}) J_{n-l}(\alpha) , \quad (22)$$

$$t_n e^{ik_n b} = \sum_l (a_l e^{q_l b} + b_l e^{-q_l b}) J_{n-l}(\alpha) , \quad (23)$$

$$ik_n t_n e^{ik_n b} = \sum_l q_l (a_l e^{q_l b} - b_l e^{-q_l b}) J_{n-l}(\alpha) . \quad (24)$$

The Floquet energy is determined from these relations by demanding nontrivial solutions of the coefficients. In practice, however, we must truncate the above equations to a finite number of side-bands, eg., $n = 0, \pm 1, \dots, \pm N$. The number N is determined by the frequency and the strength of the oscillation according to $N > V_1/\hbar\omega$ [7, 8, 17].

To determine the Floquet energy ε , we first separate the boundary conditions for the central band $n = 0$ from the other side-bands $l \neq 0$ in Eq.(21)-(24) (we set $A_0 = 1$ for simplicity):

$$\sin(k_0 a) = (a_0 e^{q_0 a} + b_0 e^{-q_0 a}) J_0(\alpha) + \sum_{l \neq 0} (a_l e^{q_l a} + b_l e^{-q_l a}) J_{-l}(\alpha), \quad (25)$$

$$k_0 \cos(k_0 a) = q_0 (a_0 e^{q_0 a} - b_0 e^{-q_0 a}) J_0(\alpha) + \sum_{l \neq 0} q_l (a_l e^{q_l a} - b_l e^{-q_l a}) J_{-l}(\alpha), \quad (26)$$

$$t_0 e^{ik_0 b} = (a_0 e^{q_0 b} + b_0 e^{-q_0 b}) J_0(\alpha) + \sum_{l \neq 0} (a_l e^{q_l b} + b_l e^{-q_l b}) J_{-l}(\alpha), \quad (27)$$

$$ik_0 t_0 e^{ik_0 b} = q_0 (a_0 e^{q_0 b} - b_0 e^{-q_0 b}) J_0(\alpha) + \sum_{l \neq 0} q_l (a_l e^{q_l b} - b_l e^{-q_l b}) J_{-l}(\alpha). \quad (28)$$

The coefficients a_l and b_l ($l \neq 0$) in Eq.(25-28) can always be related to the coefficients a_0 and b_0 as

$$a_l = f_{la}(k_0, \omega, V_1) a_0 + f_{lb}(k_0, \omega, V_1) b_0, \quad (29)$$

$$b_l = g_{la}(k_0, \omega, V_1) a_0 + g_{lb}(k_0, \omega, V_1) b_0, \quad (30)$$

where f 's and g 's are functions determined as follows. Eliminating the A_n 's and t_n 's in Eq.(21)-(24), we can obtain

$$\begin{aligned} & A_{n,n}^- e^{q_n a} J_0 a_n + A_{n,n}^+ e^{-q_n a} J_0 b_n + \sum_{l \neq n, 0} A_{n,l}^- e^{q_l a} J_{n-l} a_l + \sum_{l \neq n, 0} A_{n,l}^+ e^{-q_l a} J_{n-l} b_l \\ = & -A_{n,0}^- e^{q_0 a} J_n a_0 - A_{n,0}^+ e^{-q_0 a} J_n b_0, \end{aligned} \quad (31)$$

and

$$\begin{aligned} & B_{n,n}^+ e^{q_n b} J_0 a_n + B_{n,n}^- e^{-q_n b} J_0 b_n + \sum_{l \neq n, 0} B_{n,l}^+ e^{q_l b} J_{n-l} a_l + \sum_{l \neq n, 0} B_{n,l}^- e^{-q_l b} J_{n-l} b_l \\ = & -B_{n,0}^+ e^{q_0 b} J_n a_0 - B_{n,0}^- e^{-q_0 b} J_n b_0, \end{aligned} \quad (32)$$

where

$$A_{n,l}^\pm \equiv \cos k_n a \pm \frac{q_l}{k_n} \sin k_n a, \quad \text{and} \quad B_{n,l}^\pm \equiv 1 \pm i \frac{q_l}{k_n}. \quad (33)$$

As mentioned before, in practice a truncated version of Eqs. (31) and (32) has to be used. In a m side-bands approximation, the index n ranges from $-m$ to m except 0. Then Eqs. (31) and (32) together represent a set of $2m$ equations with $2m$ unknowns a_n and b_n . The solutions of these unknowns can then be solved by the Cramer's rule [25] in the forms of Eq.(29) and Eq.(30).

Replacing the a_l 's and b_l 's by means of Eqs.(29) and (30), one can rewrite Eqs.(25) to (28) as

$$\sin(k_0 a) = F_1(k_0; \omega, V_1) e^{q_0 a} a_0 + F_2(k_0; \omega, V_1) e^{-q_0 a} b_0, \quad (34)$$

$$k_0 \cos(k_0 a) = F_3(k_0; \omega, V_1) q_0 e^{q_0 a} a_0 - F_4(k_0; \omega, V_1) q_0 e^{-q_0 a} b_0, \quad (35)$$

$$t_0 e^{ik_0 b} = F_5(k_0; \omega, V_1) e^{q_0 b} a_0 + F_6(k_0; \omega, V_1) e^{-q_0 b} b_0, \quad (36)$$

$$ik_0 t_0 e^{ik_0 b} = F_7(k_0; \omega, V_1) q_0 e^{q_0 b} a_0 - F_8(k_0; \omega, V_1) q_0 e^{-q_0 b} b_0, \quad (37)$$

where the coefficient $F_i(k_0; \omega, V_1)$ ($i = 1, \dots, 8$) are

$$F_1(k_0; \omega, V_1) = J_0(\alpha) + e^{-q_0 a} \sum_{l \neq 0} (f_{la} e^{q_l a} + g_{la} e^{-q_l a}) J_{-l}(\alpha), \quad (38)$$

$$F_2(k_0; \omega, V_1) = J_0(\alpha) + e^{q_0 a} \sum_{l \neq 0} (f_{lb} e^{q_l a} + g_{lb} e^{-q_l a}) J_{-l}(\alpha), \quad (39)$$

$$F_3(k_0; \omega, V_1) = J_0(\alpha) + e^{-q_0 a} \sum_{l \neq 0} \frac{q_l}{q_0} (f_{la} e^{q_l a} - g_{la} e^{-q_l a}) J_{-l}(\alpha), \quad (40)$$

$$F_4(k_0; \omega, V_1) = J_0(\alpha) - e^{q_0 a} \sum_{l \neq 0} \frac{q_l}{q_0} (f_{lb} e^{q_l a} - g_{lb} e^{-q_l a}) J_{-l}(\alpha), \quad (41)$$

$$F_5(k_0; \omega, V_1) = J_0(\alpha) + e^{-q_0 b} \sum_{l \neq 0} (f_{la} e^{q_l b} + g_{la} e^{-q_l b}) J_{-l}(\alpha), \quad (42)$$

$$F_6(k_0; \omega, V_1) = J_0(\alpha) + e^{q_0 b} \sum_{l \neq 0} (f_{lb} e^{q_l b} + g_{lb} e^{-q_l b}) J_{-l}(\alpha), \quad (43)$$

$$F_7(k_0; \omega, V_1) = J_0(\alpha) + e^{-q_0 b} \sum_{l \neq 0} \frac{q_l}{q_0} (f_{la} e^{q_l b} - g_{la} e^{-q_l b}) J_{-l}(\alpha), \quad (44)$$

$$F_8(k_0; \omega, V_1) = J_0(\alpha) - e^{q_0 b} \sum_{l \neq 0} \frac{q_l}{q_0} (f_{lb} e^{q_l b} - g_{lb} e^{-q_l b}) J_{-l}(\alpha). \quad (45)$$

Then by eliminating the coefficients a_0 , b_0 and t_0 in Eqs.(34) to (37), we arrive at an equation which is a function of ε ($= \hbar^2 k_0^2 / 2m$),

$$F_4 \frac{q_0}{k_0} \tan k_0 a + F_2 = \frac{F_8 q_0 + i F_6 k_0}{F_7 q_0 - i F_5 k_0} \left(F_3 \frac{q_0}{k_0} \tan k_0 a - F_1 \right) e^{-2q_0(b-a)}. \quad (46)$$

Its solution determines the Floquet energy of the metastable system. Comparing this equation with the corresponding one for the static case, i.e. Eq.(4), we see the effect of the time-periodic potential is contained entirely in the coefficients F_i .

In the next section we will solve Eq.(46) numerically. Once the Floquet energy ε of the metastable system is determined, the probability of the particle still being trapped by the potential barrier at time $t > 0$, i.e. the non-decay probability $P(t)$, can be obtained as

$$\begin{aligned} P(t) &= \frac{\int_0^b |\Psi(x, t)|^2 dx}{\int_0^b |\Psi(x, 0)|^2 dx} \\ &= e^{2Im(\varepsilon)t/\hbar} \frac{\int_0^b |\Phi_\varepsilon(x, t)|^2 dx}{\int_0^b |\Phi_\varepsilon(x, 0)|^2 dx} \\ &\equiv e^{2Im(\varepsilon)t/\hbar} h(t), \end{aligned} \quad (47)$$

with $P(0) = 1$. The imaginary part of the Floquet energy, which enters $P(t)$ via the factor $\exp(2Im(\varepsilon)t/\hbar)$, gives a measure of the stability of the system. Unlike the static case, however, here $P(t)$ is not a monotonic function of time, owing to the time-dependent function $h(t)$. But since $h(t)$ is only a periodic function oscillating between two values which are of order one, the essential behavior of $P(t)$ at large times is still mainly governed by the exponential factor. Hence, as a useful measure of the nondecay rate of the particle in the well, we can use a coarse-grained nondecay probability $\bar{P}(t)$ defined as [17]

$$\bar{P}(t) \equiv e^{2Im(\varepsilon)t/\hbar} \langle h(t) \rangle, \quad (48)$$

where $\langle h(t) \rangle$ is the time average of $h(t)$ over one period of oscillation.

Owing to the complexity of the coefficients $F_i(k_0; \omega, V_1)$, the solution of Eq.(46) has to be obtained numerically. We shall present the numerical analysis in the next section. Here let us consider the limiting cases of our model. From the expressions of the coefficients $F_i(k_0; \omega, V_1)$ (Eq.(38) to Eq.(45)), we can easily check the coefficients $F_i(k_0; \omega, V_1)$ all approach one when the parameter $\alpha = V_1/\hbar\omega \rightarrow 0$,

$$\lim_{V_1/\hbar\omega \rightarrow 0} F_i(k_0; \omega, V_1) \rightarrow 1, \quad i = 1, \dots, 8. \quad (49)$$

Hence in the limit $V_1 \rightarrow 0$ or $\omega \rightarrow \infty$, Eq.(46) is identical to Eq.(4) in the static case, and the Floquet energy in these limits are just the complex eigenenergy of the static case. This is understandable, since in the limit $V_1 \rightarrow 0$ the potential becomes static. And at very high frequencies, the dynamical time scale of the particle in the well is much larger than the time scale of the oscillating barrier ω^{-1} , hence the height of the time-periodically oscillating barrier seen by the particle should be its time-averaged value, namely, $\langle V_0 + V_1 \cos \omega t \rangle = V_0$, which is independent of the time-oscillating part of the barrier [5].

IV. NUMERICAL ANALYSIS OF MODEL A

In this section, we will investigate the quantum metastability of Model A by finding the solutions of Eq.(46) numerically. We are interested in the metastability of the system under different amplitudes and frequencies of the oscillating barrier, since these are the experimentally controllable parameters. For definiteness, we take the barrier to have height $V_0 = 10.0$ in the atomic units (a.u.) ($e = m_e = \hbar = 1$), and boundaries at $a = 1$ and $b = 2$ (a.u.). With these parameters, there is only one solution with $Re(E) < V_0$ in the static case. This is a metastable state having complex energy $E_0/V_0 = 0.322052 - 0.000110412i$. Other solutions have $Re(E) > V_0$ and are more unstable. We shall be interested in this paper only in the coupling between the metastable state E_0 and the next higher one with $E_1/V_0 = 1.11205 - 0.025062i$. Coupling between other metastable states can be considered similarly. For the oscillating potential, we shall solve Eq.(46) numerically for cases with different oscillating amplitude V_1/V_0 and frequency ω/V_0 .

A. Comparison of 2 and 3 side-bands approximations

In this subsection we first study how good a 2 side-bands approximation is by comparing it with the 3 side-bands approximation. Floquet energy as a function of the amplitude of the oscillating barrier V_1 evaluated based on 2 side-bands (solid line) and 3 side-bands (dotted line) approximations are shown in Fig.(1) and Fig.(2) for $\omega/V_0 = 0.01$ and 0.02, respectively.

As mentioned before, if $\{\varepsilon, \Phi_\varepsilon\}$ is a solution of the Schrödinger equation, then $\{\varepsilon' = \varepsilon + n\hbar\omega, \Phi_{\varepsilon'} = \Phi_\varepsilon \exp(in\omega t)\}$ is also a solution for any integer n . And they are physically equivalent as the total wave function Ψ_ε is the same. For metastable system, this means that all Floquet states with real parts differing by $n\hbar\omega$ ($n = 0, \pm 1, \dots$) will have the same imaginary part. We have checked this for $n = 0, \pm 1$ in the 2 and 3 side-bands approximations.

Part(a) [part(b)] of Fig. 1 and 2 show the relation of the real (imaginary) part of the Floquet energy and the oscillating amplitude parameter V_1/V_0 at fixed ω . Fig. (1-a) and (2-a) show that if $Re(\varepsilon/V_0) = Re(E_0/V_0) = 0.322052$ is the Floquet energy of the system, so are the $Re(\varepsilon/V_0) \pm \omega/V_0$ for all values of V_1 less than certain limit. Fig. (1-b) and (2-b) indicate that the imaginary part of these solutions merge into one curve for $V_1/V_0 \leq 0.01$ in Fig.(1-b) and $V_1/V_0 \leq 0.02$ in Fig.(2-b). The divergence of the three curves at higher V_1 is caused by the truncation of the number of side-bands in numerical analysis. Fig.(1-b) shows that the 2 side-bands approximation is good for $V_1/V_0 \leq 0.01$ at $\omega/V_0 = 0.01$ (i.e. $\alpha \equiv V_1/\omega \leq 1$), and the 3 side-bands approximation is accurate for $V_1/V_0 \leq 0.02$ at $\omega/V_0 = 0.02$ (i.e. $\alpha \equiv V_1/\omega \leq 2$). These results are consistent with the usual requirement for the N side-bands approximation mentioned previously, namely, $\alpha \equiv V_1/\omega \leq N$ [7, 8, 17]. Similar argument for the accuracy in the approximation can also be checked in Fig.(2-b). Stability of the system is determined by the imaginary part of the Floquet energy. From part (b) of Fig. 1 and 2, we see that the imaginary part of Floquet energy increases as V_1 increases. This means that, at fixed frequency, a larger oscillating amplitude will cause the system to be less stable. On the other hand, once V_1 is reduced to zero the quantum metastability of the system will approach to the static case ($Log(-Im(\varepsilon/V_0)) = -3.95698$), because, as we explained at the end of the last section, in the limit $V_1 \rightarrow 0$ the driven system reduces to the static case.

B. Floquet energy as function of the frequency and amplitude of the oscillating field

In this subsection, we will investigate the effects of the oscillating frequency and amplitude on the quantum metastability of the system in the 2 side-bands approximation. As we have learned in the previous subsection, the 2 side-bands approximation is good enough for $\omega > V_1$ ($\alpha^{-1} > 1$).

Fig. (3-a) and (3-b) present, respectively, the relation of the real and imaginary parts of the Floquet energy and the driving frequency with the parameters $V_0 = 10.0$, $a = 1$, $b = 2$, and $V_1 = 1.0$ in the atomic units. The solutions of Eq.(46) have the form $\varepsilon = \varepsilon_0 + n\omega$ ($n = 0, \pm 1, \pm 2, \dots$), with $Re(\varepsilon_0)$ (the horizontal branch) lie close to the energies $Re(E_0)$ and $Re(E_1)$ in the static potential. That is, these branches of $Re(\varepsilon)$ emanate from either $Re(E_0)$ or $Re(E_1)$ at $\omega = 0$. Branches emerging from the same point have the same imaginary part. Numerical results show that, with the barrier oscillating, these states become less stable. For simplicity, in Fig. (3a) we show only two branches emerging from the two states with $Re(E_0)$ (solid curves for $n = 0, 1$) and $Re(E_1)$ (dotted curves for $n = 0, -1$) in the static case. As mentioned before, solutions can always be reduced to the first Floquet zone, $Re(\varepsilon)$ (modulo ω), which are points under the line $Re(\varepsilon) = \omega$.

Figure (3-b) shows that the imaginary parts of the Floquet energies of the two states fluctuate slightly as the frequency changes. At frequency close to the resonance frequency $\omega \approx \omega_R \equiv Re(E_1) - Re(E_0) \approx 0.79V_0$, a direct crossing of the real parts of the Floquet energies of the two states occurs. This is indicated by the point a in the first Floquet

zone, or equivalently, point b in the second Floquet zone. That it is a direct crossing is shown more clearly with a refined scale in Fig. (3-c) and (3-d). We see that for the first metastable state (solid curve), $Re(\varepsilon)$ exhibits around ω_R a ‘‘Fano’’ resonance pattern, where a sharp dip is followed by a peak. For the second metastable state (dotted curve), an ‘‘anti-Fano’’ pattern was seen instead. In the neighborhood of ω_R , the first metastable state becomes less unstable (point c), while the second state appears to be slightly more stable (point d). Beyond ω_R , the stability of the two states revert to their respective orders of magnitude. Similar behavior is also observed at the point of direct crossing in the system discussed in [17].

Figures 4 to 7 present similar graphs as in Fig. 3, but with $V_1/V_0 = 1.6, 1.7, 2.0$ and 4.0 , respectively (other parameters being the same). In Fig. 4 we see that, with V_1/V_0 increases up to 1.6 , the system still behaves essentially in the same way as when $V_0/V_1 = 1.0$. Only the first metastable state becomes less stable, while the second metastable state tends to be more stable at the point of direct crossing.

The behavior of the system changes qualitatively, when V_0/V_1 increases beyond a critical point. At $V_1/V_0 = 1.7$, the crossing between the two states changes from a direct crossing into an avoided crossing, as depicted in Fig. 5. Increasing V_1/V_0 further only enhances the difference of the Floquet energies at the point of avoided crossing (Fig. 6 and 7). At and beyond the avoided crossing, the two states exchange stability: the second and originally less stable state becomes more stable than the first state, which now assumes a stability which is of similar order of magnitude as that of the second state before the crossing. Such phenomenon has been previously discussed in [17].

The above results indicate the possibility of controlling stability of states in a quantum well. One may tune up the frequency adiabatically up to the point where the real parts of the Floquet energy of the two states meet. If the crossing is a direct crossing, then one can increase the magnitude of the oscillation V_1 of the barrier before the crossing until the direct crossing turns into an avoided one. When the frequency is increased further to pass beyond the avoided crossing, the two states exchange stability. Then by reducing V_1 to zero, the two states in the static well are interchanged. If the lowest energy in the static well is a stable bound state (as in the case discussed in [17]), the above procedure can turn an upper metastable state into a stable one.

V. MODEL B: THE STATIC MODEL WITH A TIME-PERIODICALLY OSCILLATING BOTTOM

Let us now consider a variant of the above model, namely, the static model with a time-periodically oscillating bottom instead of an oscillating barrier. The potential can be expressed as

$$V(x, t) = \begin{cases} \infty, & x < 0, \\ V_1 \cos(\omega t), & 0 \leq x < a, \\ V_0, & a \leq x \leq b, \\ 0, & x > b. \end{cases} \quad (50)$$

The wave function inside the barrier well, i.e., $0 \leq x \leq a$, can be obtained by the similar procedure as in Sect. III, except that we have to impose the boundary condition $\Psi'_I(x=0, t) = 0$ in this case. The result is

$$\begin{aligned} \Psi'_I(x, t) &= \sum_l \sum_n A'_n \sin(k_n x) J_{l-n}(\alpha) e^{-i(\varepsilon + l\hbar\omega)t/\hbar}, \\ &= \sum_l \sum_n A'_n \sin(k_n x) J_{l-n}(\alpha) e^{-iE_l t/\hbar}, \end{aligned} \quad (51)$$

where $k_n = \sqrt{2m(\varepsilon + n\hbar\omega)}/\hbar$. Continuity of the wave function at the boundaries $x = a$ and b requires that the wave function has the form

$$\Psi'_{II}(x, t) = \sum_l (a'_l e^{q_l x} + b'_l e^{-q_l x}) e^{-iE_l t/\hbar} \quad (52)$$

in the region $a \leq x < b$, where $q_l = \sqrt{2m(V_0 - \varepsilon - l\hbar\omega)}/\hbar$, and

$$\Psi'_{III}(x, t) = \sum_l t'_l e^{ik_l x} e^{-iE_l t/\hbar}, \quad (53)$$

in the region $x \geq b$, where the Gamow’s outgoing wave boundary condition has been imposed.

The relations among the coefficients A'_n, a'_n, b'_n and t'_n can be obtained by matching the boundary conditions at $x = a$ and b . This leads to

$$\sum_n A'_n \sin(k_n a) J_{l-n}(\alpha) = a'_l e^{q_l a} + b'_l e^{-q_l a}, \quad (54)$$

$$\sum_n k_l A'_n \cos(k_n a) J_{l-n}(\alpha) = q_l (a'_l e^{q_l a} - b'_l e^{-q_l a}) , \quad (55)$$

$$t'_l e^{i k_l b} = a'_l e^{q_l b} + b'_l e^{-q_l b} , \quad (56)$$

$$i k_l t'_l e^{i k_l b} = q_l (a'_l e^{q_l b} - b'_l e^{-q_l b}) , \quad (57)$$

Eliminating t'_l from Eq.(56) and Eq.(57) gives the relation between a'_l and b'_l ,

$$b'_l = -\frac{1 + i q_l / k_l}{1 - i q_l / k_l} e^{2 q_l b} a'_l . \quad (58)$$

Using this relation to replace b'_l in Eq.(54) and Eq.(55), we obtain

$$\sum_n A'_n \sin(k_n a) J_{l-n}(\alpha) = e^{q_l b} \left(e^{-q_l(b-a)} - \frac{1 + i q_l / k_l}{1 - i q_l / k_l} e^{q_l(b-a)} \right) a'_l , \quad (59)$$

and

$$\sum_n A'_n k_n \cos(k_n a) J_{l-n}(\alpha) = q_l e^{q_l b} \left(e^{-q_l(b-a)} + \frac{1 + i q_l / k_l}{1 - i q_l / k_l} e^{q_l(b-a)} \right) a'_l , \quad (60)$$

respectively. These two equations can be combined by eliminating the coefficients a'_l , giving

$$\sum_n \left[A_{n,l}^- e^{-q_l(b-a)} - \frac{B_{l,l}^+}{B_{l,l}^-} A_{n,l}^+ e^{q_l(b-a)} \right] k_n J_{l-n}(\alpha) A'_n = 0 , \quad (61)$$

where the notation $A_{n,l}^\pm$ and $B_{n,l}^\pm$ are as defined in Model A, Eq. (33).

We now show how to determine the Floquet energy of the metastable system from Eq.(61). For a general amplitude $V_1 \neq 0$, Eq.(61) in the m side-bands approximation is

$$\sum_{n=-m}^m \left[A_{n,l}^- e^{-q_l(b-a)} - \frac{B_{l,l}^+}{B_{l,l}^-} A_{n,l}^+ e^{q_l(b-a)} \right] k_n J_{l-n}(\alpha) A'_n = 0 . \quad (62)$$

Moving the term with the coefficient A'_0 of the above equation to the right-hand side, we get

$$\begin{aligned} & \sum_{\substack{n=-m \\ n \neq 0}}^m \left[A_{n,l}^- e^{-q_l(b-a)} - \frac{B_{l,l}^+}{B_{l,l}^-} A_{n,l}^+ e^{q_l(b-a)} \right] k_n J_{l-n}(\alpha) A'_n \\ & = - \left[A_{0,l}^- e^{-q_l(b-a)} - \frac{B_{l,l}^+}{B_{l,l}^-} A_{0,l}^+ e^{q_l(b-a)} \right] k_0 J_l(\alpha) A'_0 , \end{aligned} \quad (63)$$

The left-hand side of the equation contains $2m$ unknown coefficients $A'_{n \neq 0}$. As the total number of side-band is also $2m$ ($l = \pm 1, \dots, \pm m$), it is sufficient to use the Cramer's rule to obtain the relation

$$A'_{n \neq 0} = C_n(\varepsilon, V_1, \omega) A'_0 \quad (64)$$

with $C_0 = 1$. We now insert this representation of $A'_{n \neq 0}$ into Eq.(62). Eq.(62) for the central band ($l = 0$) becomes

$$\left\{ \sum_{n=-m}^m \left[A_{n,0}^- e^{-q_0(b-a)} - \frac{B_{0,0}^+}{B_{0,0}^-} A_{n,0}^+ e^{q_0(b-a)} \right] k_n J_{-n}(\alpha) C_n \right\} A'_0 = 0 . \quad (65)$$

Nontrivial solution of A'_0 , i.e. $A'_0 \neq 0$, requires that

$$\sum_{n=-m}^m \left[A_{n,0}^- e^{-q_0(b-a)} - \frac{B_{0,0}^+}{B_{0,0}^-} A_{n,0}^+ e^{q_0(b-a)} \right] k_n J_{-n}(\alpha) C_n = 0 . \quad (66)$$

The Floquet energy of the metastable system ε can then be determined by finding the solutions of this equation.

Let us mention briefly the limiting case in which $V_1 \rightarrow 0$ (i.e., $\alpha \rightarrow 0$). Since $J_0(\alpha = 0) = 1$ and $J_{l \neq 0}(\alpha = 0) = 0$, Eq.(66) reduces to

$$A_{0,0}^- e^{-q_0(b-a)} - \frac{B_{0,0}^+}{B_{0,0}^-} A_{0,0}^+ e^{q_0(b-a)} = 0, \quad (67)$$

which, as we expect, is just the result of the static case

$$\frac{q_0 + ik_0}{q_0 - ik_0} \left(\frac{q_0}{k_0} \tan k_0 a - 1 \right) e^{-2q_0(b-a)} = \frac{q_0}{k_0} \tan k_0 a + 1. \quad (68)$$

We had solved Eq.(66) numerically for the Floquet energy of the system. To our surprise, the functional dependence of the Floquet spectrum on the amplitude and the frequency of the oscillation turns out to be exactly the same as that of Model A. Since the sets of equations of boundary conditions determining the Floquet energy are so different in form for the two models, that they should give exactly the same solutions can be of no coincidence. This prompted us to search for the underlying connection between the two models. After some efforts we eventually realize that these models are related by a discrete transform in the sense that Eqs. (21)-(24) can be transformed into Eqs. (54)-(57), and vice versa, by the discrete transform to be described below. Since Eq. (22) [(55)] and Eq. (24) [(57)] are obtainable from Eq. (21) [(54)] and Eq. (23) [(56)] by differentiation with respect to the parameters a and b , respectively, it suffices to show the transformations between Eqs. (21) and (54), and between Eqs. (23) and (56). This will be discussed in the next section. More recently, we have also realized that the underlying physics responsible for the equivalence of the two models is the gauge equivalence of the models, which we shall present in Sect VII.

VI. DISCRETE TRANSFORM

The aforementioned discrete transform is defined as follows. Consider an infinite discrete sequence $\{g_n\} = \{\dots, g_{-1}, g_0, g_1, \dots\}$ of complex numbers g_n ($n = -\infty, \dots, \infty$) with finite norms. Let us form another sequence $\{g'_n\}$ by the following transform based on the Bessel functions $J_k(\alpha)$ with integral order k and argument α :

$$\begin{aligned} g'_l(\alpha) &:= \mathcal{H}_l[\{g_n\}, \alpha] \\ &\equiv \sum_{n=-\infty}^{\infty} (-1)^n g_n J_{l-n}(\alpha), \quad n = 0, \pm 1, \pm 2, \dots \end{aligned} \quad (69)$$

This transform has the interesting property that its inverse transform is given by the same transform, i.e. the sequence $\{g_n\}$ is obtainable from $\{g'_n\}$ by the same transformation:

$$\begin{aligned} g_n &= \mathcal{H}_n[\{g'_l\}, \alpha] \\ &= \sum_{l=-\infty}^{\infty} (-1)^l g'_l J_{n-l}(\alpha). \end{aligned} \quad (70)$$

To prove this, let us substitute Eq.(69) into the right-hand side of Eq. (70). This gives

$$\begin{aligned} &\sum_{l=-\infty}^{\infty} (-1)^l g'_l J_{n-l}(\alpha) \\ &= \sum_{l=-\infty}^{\infty} (-1)^l \left[\sum_{m=-\infty}^{\infty} (-1)^m g_m J_{l-m}(\alpha) \right] J_{n-l}(\alpha) \\ &= \sum_{m=-\infty}^{\infty} (-1)^m g_m \sum_{l=-\infty}^{\infty} (-1)^l J_{l-m}(\alpha) J_{n-l}(\alpha) \\ &= \sum_{m=-\infty}^{\infty} (-1)^{m+n} g_m \sum_{l=-\infty}^{\infty} J_{l-m}(\alpha) J_{l-n}(\alpha). \end{aligned} \quad (71)$$

In obtaining the last line in Eq. (71), we have made use of the property $J_{n-l}(\alpha) = (-1)^{n-l} J_{l-n}(\alpha)$. To proceed further, we make use of a version of the addition theorems of the Bessel functions, namely [24],

$$\sum_{k=-\infty}^{\infty} J_{k+\nu}(\alpha_1) J_k(\alpha_2) = J_\nu(\alpha_1 - \alpha_2). \quad (72)$$

It is easy to prove that this theorem leads to the following interesting identity for Bessel functions with integral orders:

$$\begin{aligned} \sum_{l=-\infty}^{\infty} J_{l-m}(\alpha) J_{l-n}(\alpha) &= J_{m-n}(0) \\ &= \delta_{mn} . \end{aligned} \quad (73)$$

Using Eq. (73), Eq. (71) becomes g_n , which is exactly the left-hand side of Eq. (70).

Let us now apply the transform to Eq. (54). We get

$$(-1)^n A'_n \sin(k_n a) = \sum_l (-1)^l (a'_l e^{q_l a} + b'_l e^{-q_l a}) J_{n-l}(\alpha) . \quad (74)$$

We recognize that this is the same equation, Eq. (21), satisfied by A_n , a_n and b_n , with the same Floquet energy ε and frequency ω . This implies that the two sets of coefficients are related by

$$A_n = (-1)^n A'_n , \quad a_n = (-1)^n a'_n , \quad b_n = (-1)^n b'_n . \quad (75)$$

Similarly, by applying the transform to Eq. (21), we get Eq. (54) with the same connections, namely, Eq. (75), among the coefficients. With this connection of the coefficients it is seen that Eqs. (21) and (54) are dual pairs under the \mathcal{H} transform.

Now consider the transform of Eq. (56). With Eq. (75), we get

$$\begin{aligned} \sum_l (-1)^l t'_l e^{ik_l b} J_{n-l}(\alpha) &= \sum_l (-1)^l (a'_l e^{q_l b} + b'_l e^{-q_l b}) J_{n-l}(\alpha) , \\ &= \sum_l (a_l e^{q_l b} + b_l e^{-q_l b}) J_{n-l}(\alpha) . \end{aligned} \quad (76)$$

This is the same as Eq. (23) with the same Floquet energy and frequency, provided that the coefficients t_n and t'_n are related by the \mathcal{H} -transform in the following forms:

$$\begin{aligned} t_n e^{ik_n b} &= \sum_{l=-\infty}^{\infty} (-1)^l t'_l e^{ik_l b} J_{n-l}(\alpha) , \\ t'_n e^{ik_n b} &= \sum_{l=-\infty}^{\infty} (-1)^l t_l e^{ik_l b} J_{n-l}(\alpha) . \end{aligned} \quad (77)$$

The above discussions show that, the two models are mapped into one another under the \mathcal{H} -transform, with the relevant coefficients in the wave functions being related through Eqs. (75) and (77). Hence the Floquet energy spectra as function of oscillation's amplitude and frequency of the two models are identical. The wave functions, however, are different, since they have different forms, namely, Eqs. (18)-(20) for Model A, and Eqs. (51)-(53) for Model B. Nevertheless, it turns out that the relations between their coefficients in the region $0 \leq x \leq b$, where the particle is confined, can be understood as the result of a gauge transformation of the two wave functions. This will be discussed in the next section.

VII. GAUGE EQUIVALENCE OF THE TWO MODELS

In this section we show the underlying connection between the two models based on gauge invariance principle.

One needs only to consider the region in $0 < x \leq b$, since the metastable system in these two models is mainly confined within this region. The region $x > b$ does not affect the essential physics underlying the two models. This is because for a metastable state, its wave function is extremely small (nearly identical to zero, as confirmed numerically) in the region $x > b$ before the system has actually decayed. This region serves only as an ideal drain.

The gauge transformation of a quantum system with an x -independent gauge function $\chi(t)$ is given by:

$$\begin{aligned} \psi(x, t) &\rightarrow \psi' = e^{\frac{i}{\hbar}\chi(t)} \psi(x, t) , \\ V(x, t) &\rightarrow V'(x, t) = V - \frac{\partial}{\partial t} \chi(t) . \end{aligned} \quad (78)$$

When the gauge function $\chi(t)$ is chosen to be

$$\chi(t) = \frac{V_1}{\omega} \sin(\omega t) , \quad (79)$$

the potential in region $0 \leq x \leq b$ in Model A, Eq. (5), is transformed into

$$V'(x, t) = \begin{cases} -V_1 \cos(\omega t) , & 0 \leq x < a , \\ V_0 , & a \leq x \leq b . \end{cases} \quad (80)$$

This potential is physically equivalent to the potential describing Model B in the same region: they only differ in the origin of the time variable t by an amount π/ω . Hence, the potentials of the two models are related by a gauge transformation with gauge function Eq. (79) and a time shift $t \rightarrow t + \pi/\omega$.

We now examine the connection between the wave functions of the two models in the regions considered. Under the gauge transformation described by Eqs. (78) and (79), the wave function of Model A transforms according to

$$\Psi(x, t) \rightarrow \Psi' = e^{iV_1 \sin(\omega t)/\hbar\omega} \Psi(x, t) , \quad (81)$$

with

$$e^{iV_1 \sin(\omega t)/\hbar\omega} = \sum_{m=-\infty}^{\infty} (-1)^m J_m(\alpha) e^{-im\omega t} \quad (82)$$

which can be easily obtained from Eq. (11) by changing V_1 to $-V_1$ and using the fact $J_n(-\alpha) = (-1)^n J_n(\alpha)$. According to the previous discussion, we shall make the shift $t \rightarrow t + \pi/\omega$ in Ψ' and compare the resulted wave function $\Psi'(x, t + \pi/\omega)$ with that of Model B.

First we consider the region $0 \leq x \leq a$. The wave function of Model A in this region, Eq (19), is gauge-transformed into

$$\begin{aligned} \Psi'_I(x, t) &= e^{iV_1 \sin(\omega t)/\hbar\omega} \sum_n A_n \sin(k_n x) e^{-iE_n t/\hbar} \\ &= \sum_m \sum_n (-1)^m J_m(\alpha) A_n \sin(k_n x) e^{-i(\varepsilon + (n+m)\hbar\omega)t} \\ &= \sum_n \sum_l (-1)^{l-n} J_{l-n}(\alpha) A_n \sin(k_n x) e^{-iE_l t/\hbar} . \end{aligned} \quad (83)$$

In the last line of Eq. (83) the index m is changed to $m = l - n$, and $E_l = \varepsilon + (m + n)\hbar\omega$. With the shift $t \rightarrow t + \pi/\omega$, the time-dependent factor in Eq. (83) picks up a factor $\exp(-iE_l t/\hbar) = (-1)^l \exp(-i\pi\varepsilon/\hbar\omega)$. Accordingly the wave function is shifted to

$$\begin{aligned} \Psi''_I(x, t) &\equiv \Psi'(x, t + \pi/\omega) \\ &= e^{-i\pi\varepsilon/\hbar\omega} \sum_l \sum_n (-1)^n A_n \sin(k_n x) J_{l-n}(\alpha) e^{-iE_l t/\hbar} . \end{aligned} \quad (84)$$

It is now clear that the wave function Ψ''_I in Eq. (84) is equivalent, up to an irrelevant phase factor, to Ψ'_I of Model B, Eq. (51), with the identification of $A'_n = (-1)^n A_n$ as discovered in the last section.

Now we turn to the wave functions in region $a \leq x \leq b$. The relevant wave function of Model A, Eq. (18), is gauge-transformed to

$$\begin{aligned} \Psi'_II(x, t) &= \sum_m \sum_n \sum_l (-1)^m (a_l e^{q_l x} + b_l e^{-q_l x}) J_{n-l}(\alpha) J_m(\alpha) e^{-i(E_n + m\hbar\omega)t/\hbar} \\ &= \sum_k \sum_n \sum_l (a_l e^{q_l x} + b_l e^{-q_l x}) J_{n-l}(\alpha) J_{n-k}(\alpha) e^{-iE_k t/\hbar} , \end{aligned} \quad (85)$$

where we have used $J_{-m}(\alpha) = (-1)^m J_m(\alpha)$, and relabeled the index in the last expression. By making the same shift in the time variable, the wave function changes to

$$\begin{aligned} \Psi''_II(x, t) &\equiv \Psi'_II(x, t + \pi/\omega) \\ &= e^{-i\pi\varepsilon/\hbar\omega} \sum_k \sum_l (-1)^k (a_l e^{q_l x} + b_l e^{-q_l x}) e^{-iE_k t/\hbar} \sum_n J_{n-l}(\alpha) J_{n-k}(\alpha) . \end{aligned} \quad (86)$$

The sum over n in the last factor is simply the Kronecker delta symbol δ_{lk} according to Eq. (73). Hence

$$\Psi''_{II}(x, t) = e^{-i\pi\varepsilon/\hbar\omega} \sum_l (-1)^l (a_l e^{q_l x} + b_l e^{-q_l x}) e^{-iE_l t/\hbar}. \quad (87)$$

Again, up to the irrelevant phase factor, the wave function Ψ''_{II} is equivalent to Ψ'_{II} of Model B, with $a'_l = (-1)^l a_l$ and $b'_l = (-1)^l b_l$ as before.

The gauge equivalence of the wave functions of the two Models in the physically relevant regions provides a physical understanding of the identity of their Floquet spectra.

Finally, we note here that from such gauge invariance argument it also follows that the static problem is equivalent to the problem with the bottom of the well and the top of the barrier oscillating in phase with the same frequency and amplitude.

VIII. SUMMARY

In this paper we investigate the stability of a particle trapped in between an infinite wall and square barrier, with either a time-periodically oscillating barrier or bottom of the well. In these models we do not restrict the amplitude of the time-periodically oscillating potential to be small, so a nonperturbative approach based on the Floquet theory is adopted to tackle the problem. For each case we derive an equation to determine the Floquet energy of the system. The imaginary part of the Floquet energy can be used as a measure of the stability of the system. It is found that in general the oscillating field causes a quantum metastable state to decay faster. But when the Floquet energies (real part) of two states make a direct crossing, the more stable of the two states will undergo a resonance-enhanced decay, whereas the less stable state is slightly stabilized near the resonance frequency. Beyond the resonance frequency, the states resume stability of the original order of magnitude. However, if the crossing is an avoided one, the two states will switch stability: the less (more) stable state becomes more (less) stable. This gives the possibility to stabilize a metastable state, as discussed in [17]. Here we further found that when the amplitude of the oscillating potential is increased, a direct crossing could change into an avoided one. Thus, our results show that one can manipulate the stability of different states in a quantum potential by a combination of adiabatic changes of the frequency and the amplitude of the oscillating barrier. The two models we considered here were found to have identical Floquet energy spectrum for the same frequency and amplitude of the oscillating field. This was explained by a discrete transform which connects the equations of boundary conditions of the two models, and by a gauge transformation which maps the wave functions of the two models. These arguments also guarantee that the model discussed in [17] will have the same Floquet spectrum, whether the oscillating part is the barrier or the bottom of the well.

Acknowledgments

This work was supported in part by the National Science Council of the Republic of China through Grant No. NSC 92-2112-M-032-015 and NSC 93-2112-M-032-009. We would like to thank the referee for a very enlightening comment which inspired us to prove the gauge equivalence of the systems discussed here.

-
- [1] J.H. Eberly and K.C. Kulander, *Science* **262**, 1229 (1993).
 - [2] Q. Su, B.P. Irving, C.W. Johnson and J.H. Eberly, *J. Phys. B* **29**, 5755 (1996).
 - [3] N.J. van Druten, R.C. Constantinescu, J.M. Schins, H. Nieuwenhuize and H.G. Muller, *Phys. Rev. A* **55**, 622 (1997); S. Geltman and M. Fotino, *astro-ph/0203140*.
 - [4] C. Figueira de Morisson Faria, A. Fring and R. Schrader, *Laser Phys.* **9**, 379 (1999).
 - [5] M. Büttiker and R. Landauer, *Phys. Rev. Lett.* **49**, 1739 (1982).
 - [6] M. Wagner, *Phys. Rev. B* **49**, 16544 (1994); *Phys. Rev. A* **51**, 798 (1995); *Phys. Rev. Lett.* **51**, 4010 (1996).
 - [7] P.F. Berman, E.N. Bulgakov, D.K. Campbell, and A.F. Sadreev, *Physica* **B225**, 1 (1996).
 - [8] W. Li and L.E. Reichl, *Phys. Rev. B* **60**, 15 732 (1999).
 - [9] M. Henseler, T. Dittrich and K. Richter, *Phys. Rev. E* **64**, 046218 (2001).
 - [10] F. Grossmann, T. Dittrich, P. Jung and P. Hänggi, *Phys. Rev. Lett.* **67**, 516 (1991).
 - [11] M. Grifoni and P. Hänggi, *Phys. Rep.* **304**, 229 (1998).

- [12] A.H. Guth, Phys. Rev. D **23**, 347 (1981); D. La and P.J. Steinhardt, Phys. Rev. Lett. **62**, 376 (1989).
- [13] C.C. Lee and C.L. Ho, Phys. Rev. A **65**, 022111 (2002).
- [14] M.V. Berry and G. Klein, J. Phys. A **17**, 1805 (1984).
- [15] M.P.A.Fisher, Phys. Rev. B **37**, 75 (1988).
- [16] D. Sokolovski, Phys. Lett. A **132**, 381 (1988).
- [17] C.L. Ho and C.C. Lee, Phys. Rev. A **71**, 012102 (2005).
- [18] C. Liu and Q. Niu, Phys. Rev. B **47**, 13031 (1993).
- [19] A. Bohm, M. Gadella, and G.B. Mainland, Am. J. Phys. **57**, 1103 (1989).
- [20] G. Gamow, Z. Phys. **51**, 204 (1928).
- [21] R.W. Curney and E.U. Condon, Phys. Rev. **33**, 127 (1929).
- [22] A. Bohm, Quantum Mechanics : Foundations and Applications, 3rd. Ed. (Springer-Verlag, New York, 1994).
- [23] H. Sambe, Phys. Rev. A **7**, 2203 (1973).
- [24] M. Abramowitz and I.A. Stegun, Handbook of Mathematical Functions (Dover, New York, 1970).
- [25] M.L. Boas, Mathematical Methods in the Physical Sciences, 2nd. Ed. (John Wiley & Sons, 1983).

Figure Captions

Figure 1. Relation of the real (a) and imaginary (b) parts of the Floquet energy vs. the parameter V_1/V_0 at fixed frequency parameter $\omega/V_0 = 0.01$ for $V_0 = 10.0, a = 1.0, b = 2.0$ (*a.u.*). Solid and dotted lines represent the values evaluated in the 2 side-bands and 3 side-bands approximation, respectively. Values of V_1/V_0 in (b) beyond which the lines diverge indicate the points of breakdown of the respective approximations.

Figure 2. Same plots as Fig. 1 for $V_0 = 10.0, a = 1.0, b = 2.0$ (*a.u.*) and the fixed frequency parameter $\omega/V_0 = 0.02$.

Figure 3. Relation of the real and imaginary parts of the Floquet energy vs. the the driving frequency ω/V_0 for $V_0 = 10.0, V_1 = 1.0, a = 1.0$ and $b = 2.0$ (*a.u.*). Fig. (a) and (b) show the real and imaginary parts, respectively, of the Floquet energy. Fig. (c) and (d) depict the real part of the Floquet energy of the lower and the upper state, respectively, at the direct crossing with a refined scale.

Figure 4. Same plots as Fig. 3, but with $V_1 = 1.6$ (*a.u.*).

Figure 5. Same plots as Fig. 3 with $V_1 = 1.7$ (*a.u.*). Note that the crossing has become an avoided one.

Figure 6. Same plots as Fig. 5 with $V_1 = 2.0$ (*a.u.*).

Figure 7. Same plots as Fig. 3, but with $V_1 = 4.0$ (*a.u.*). The avoided crossing is enhanced.

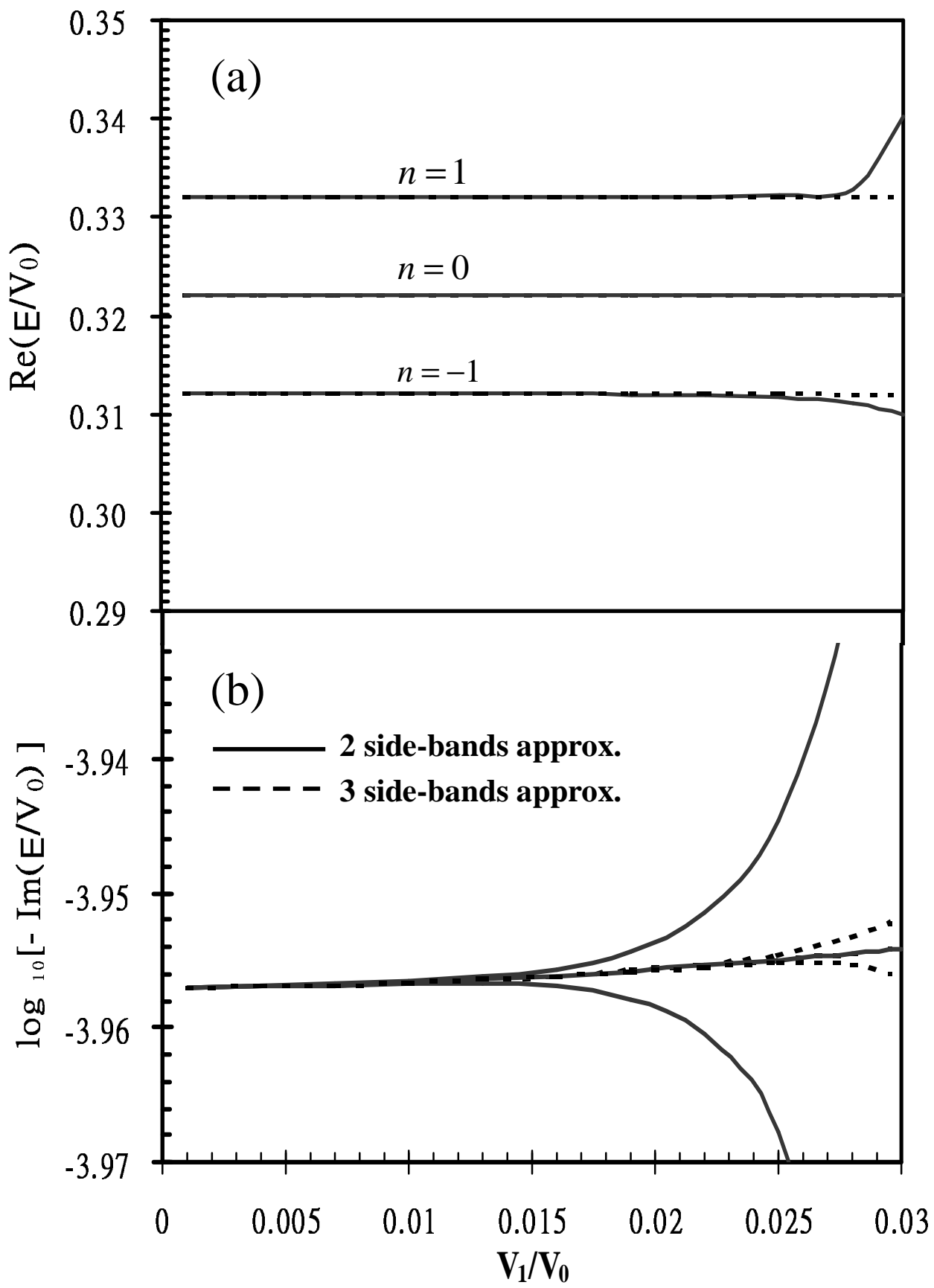


Fig.1

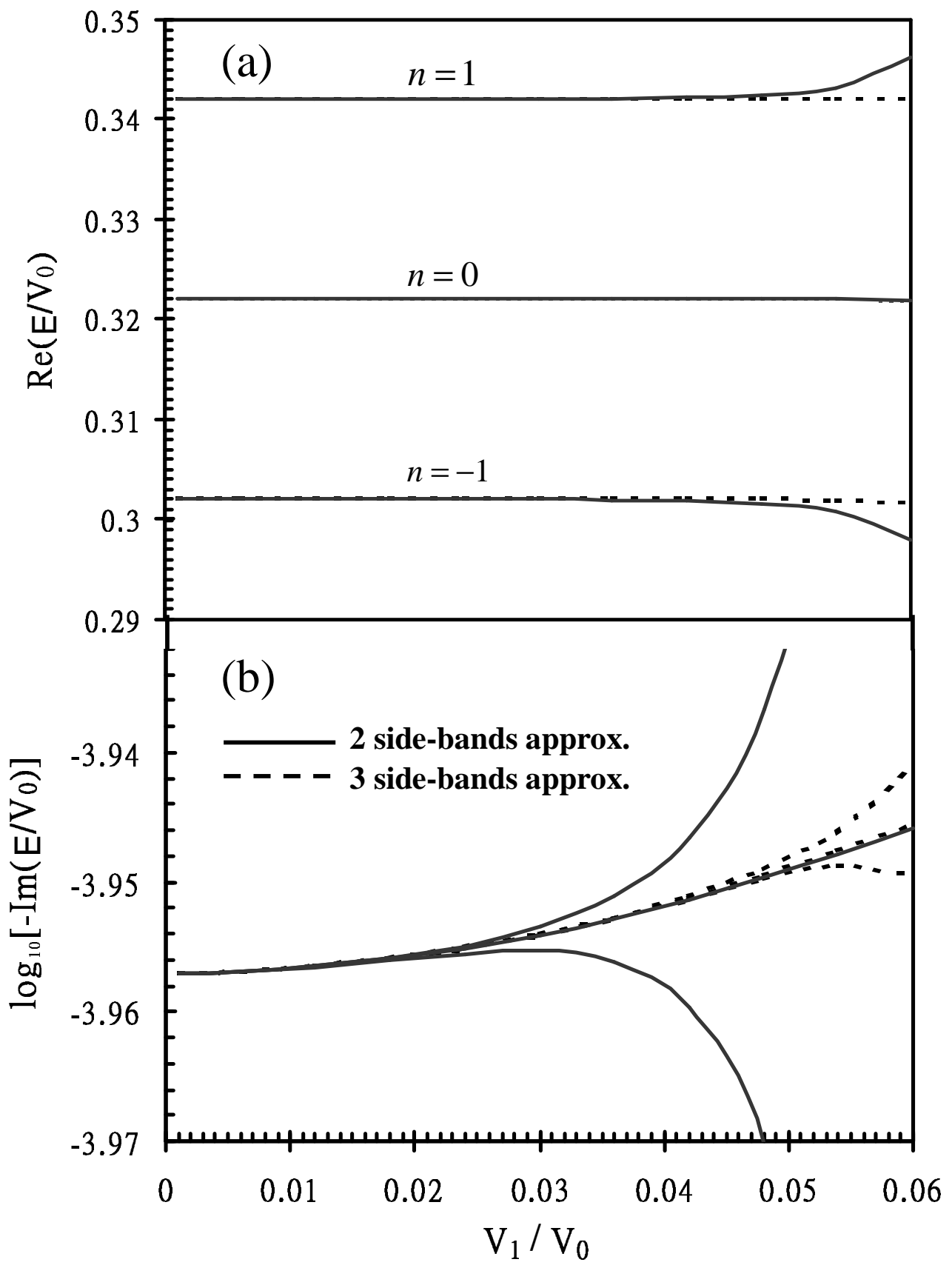


Fig.2

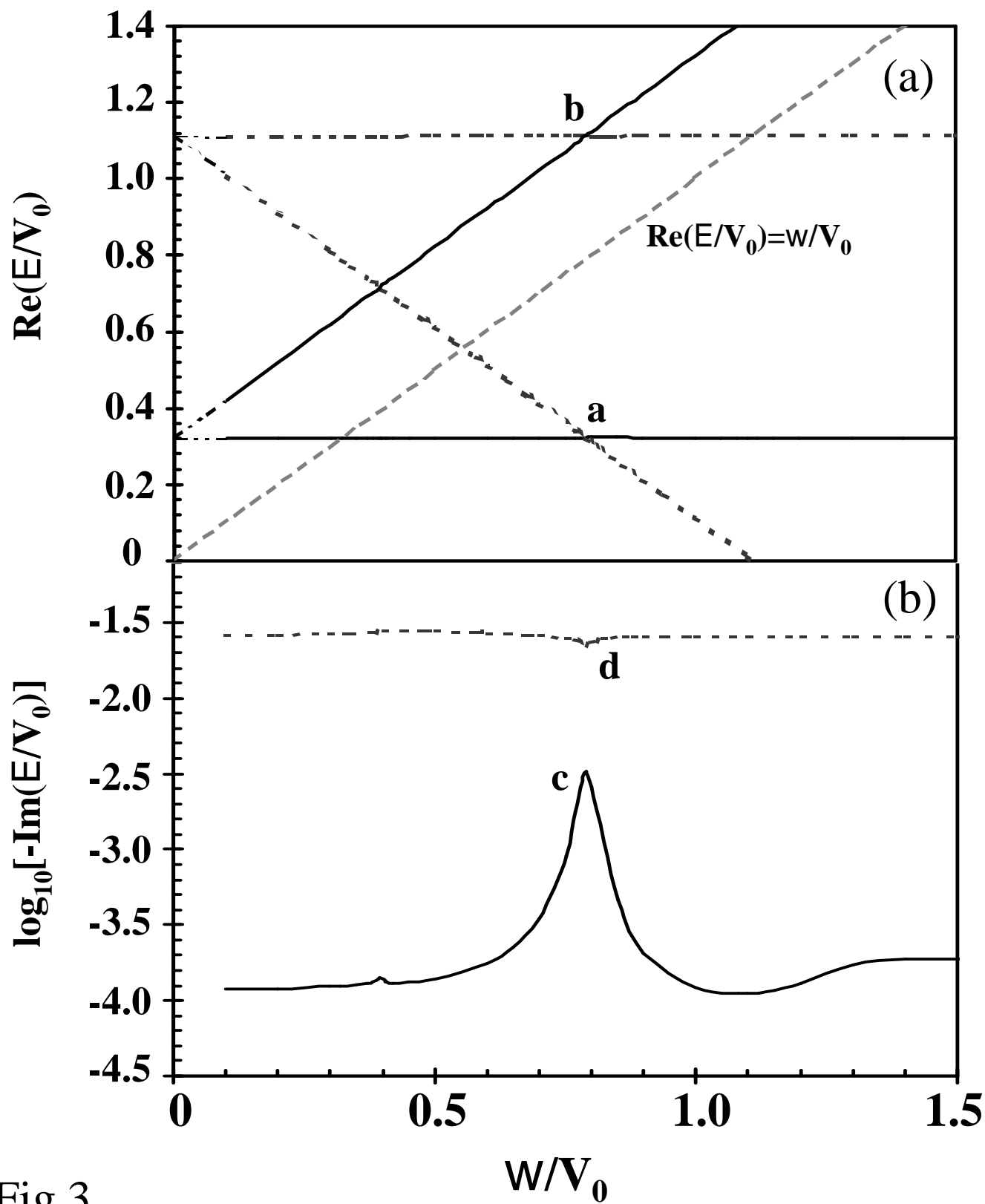


Fig.3

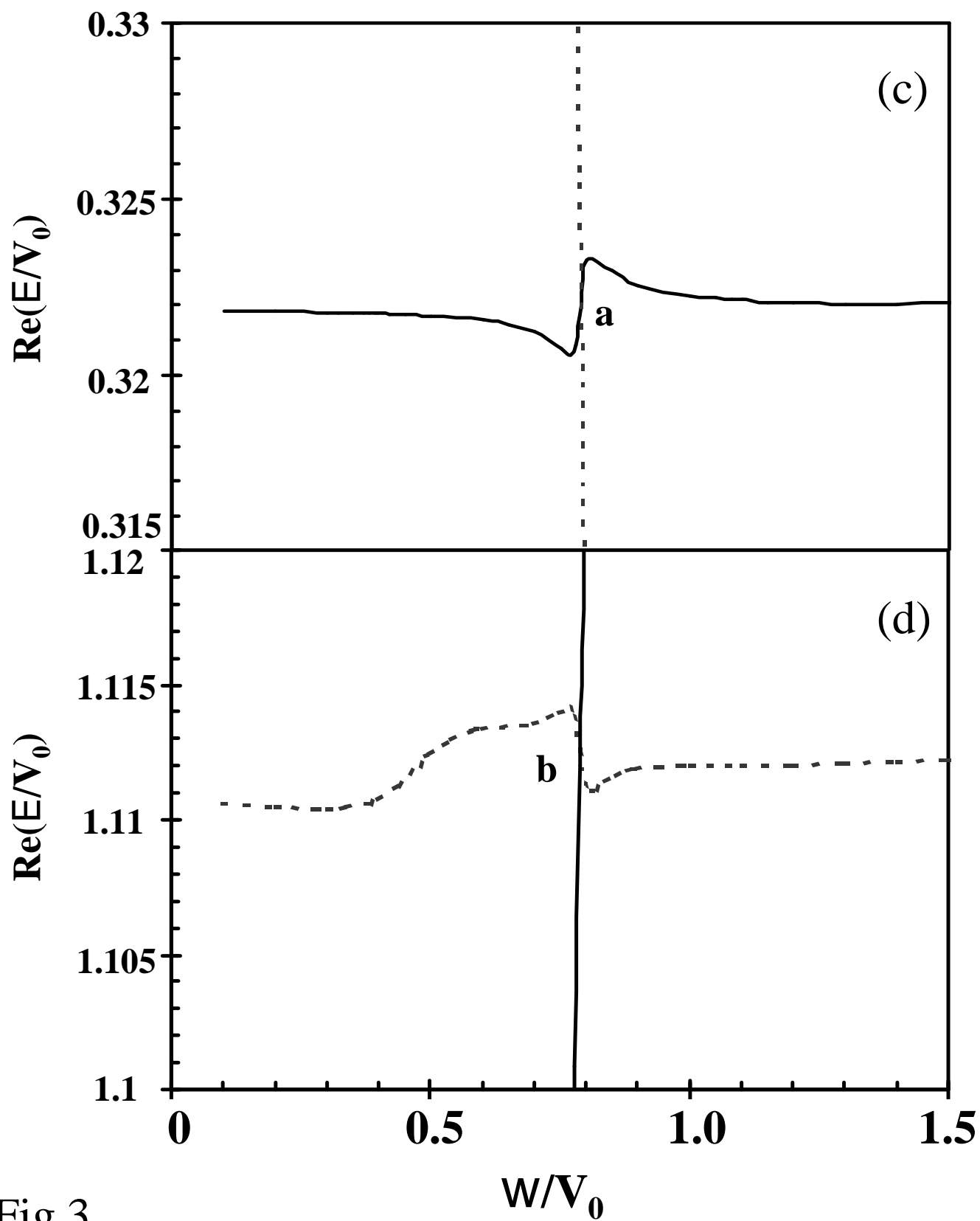


Fig.3

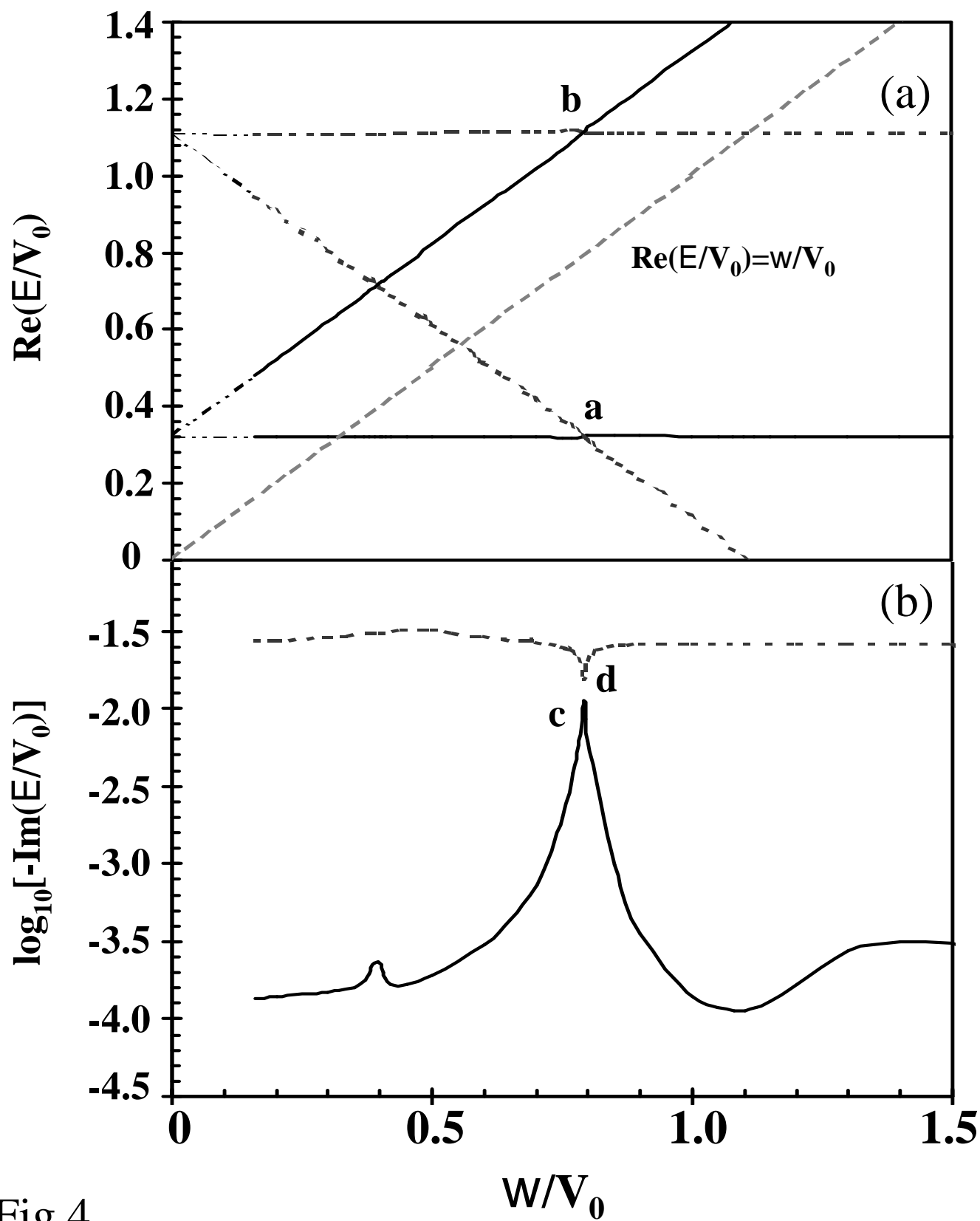


Fig.4

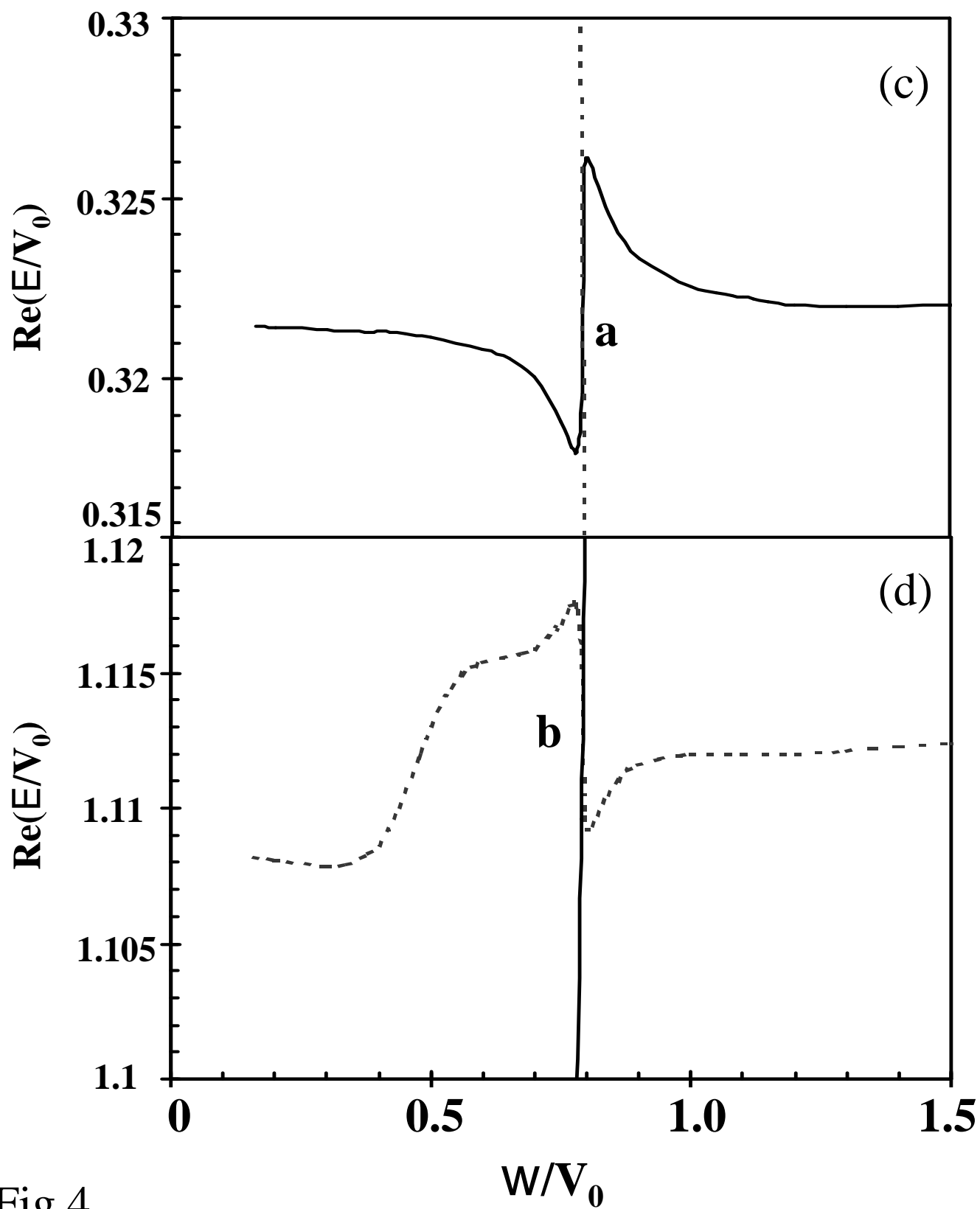


Fig.4

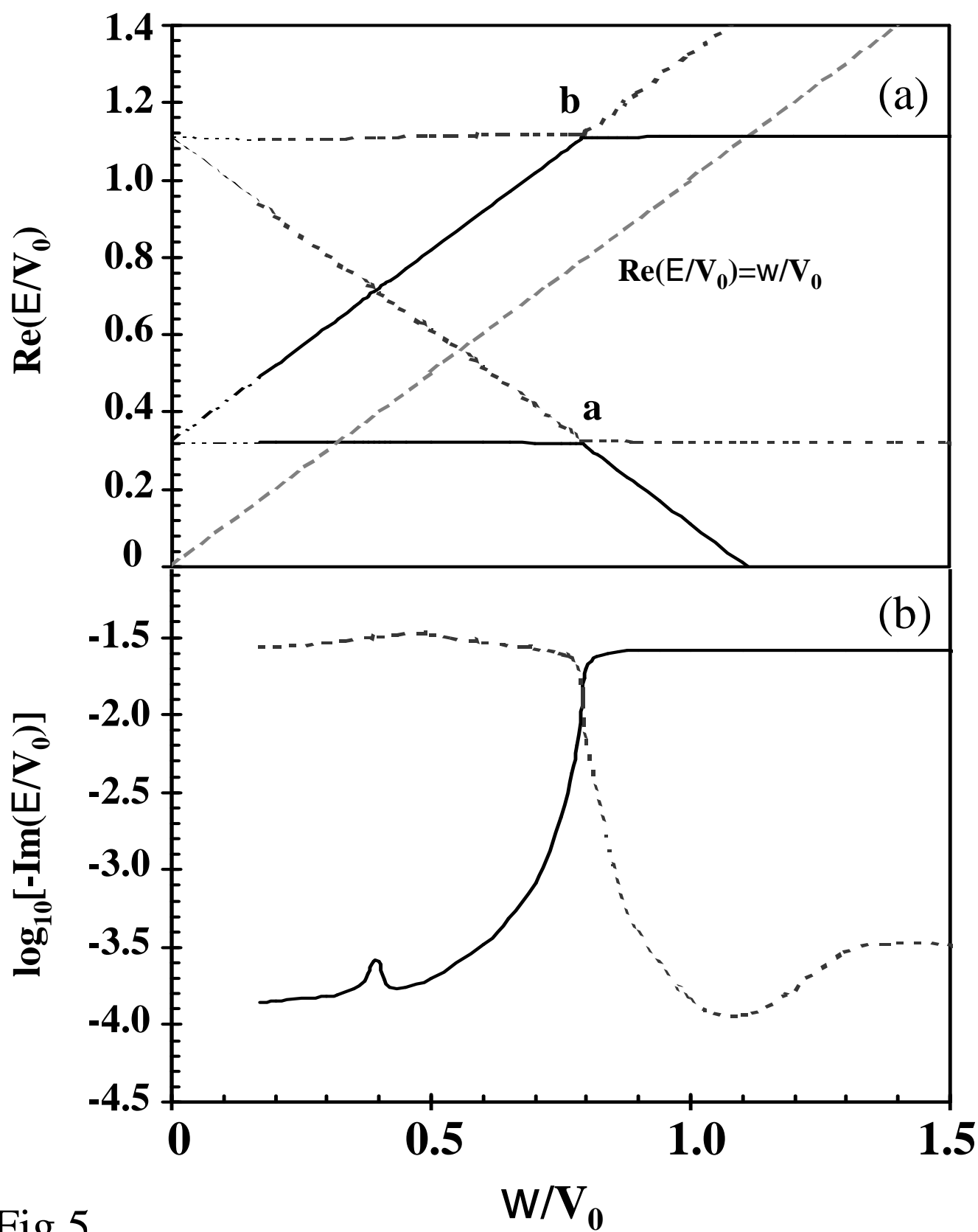


Fig.5

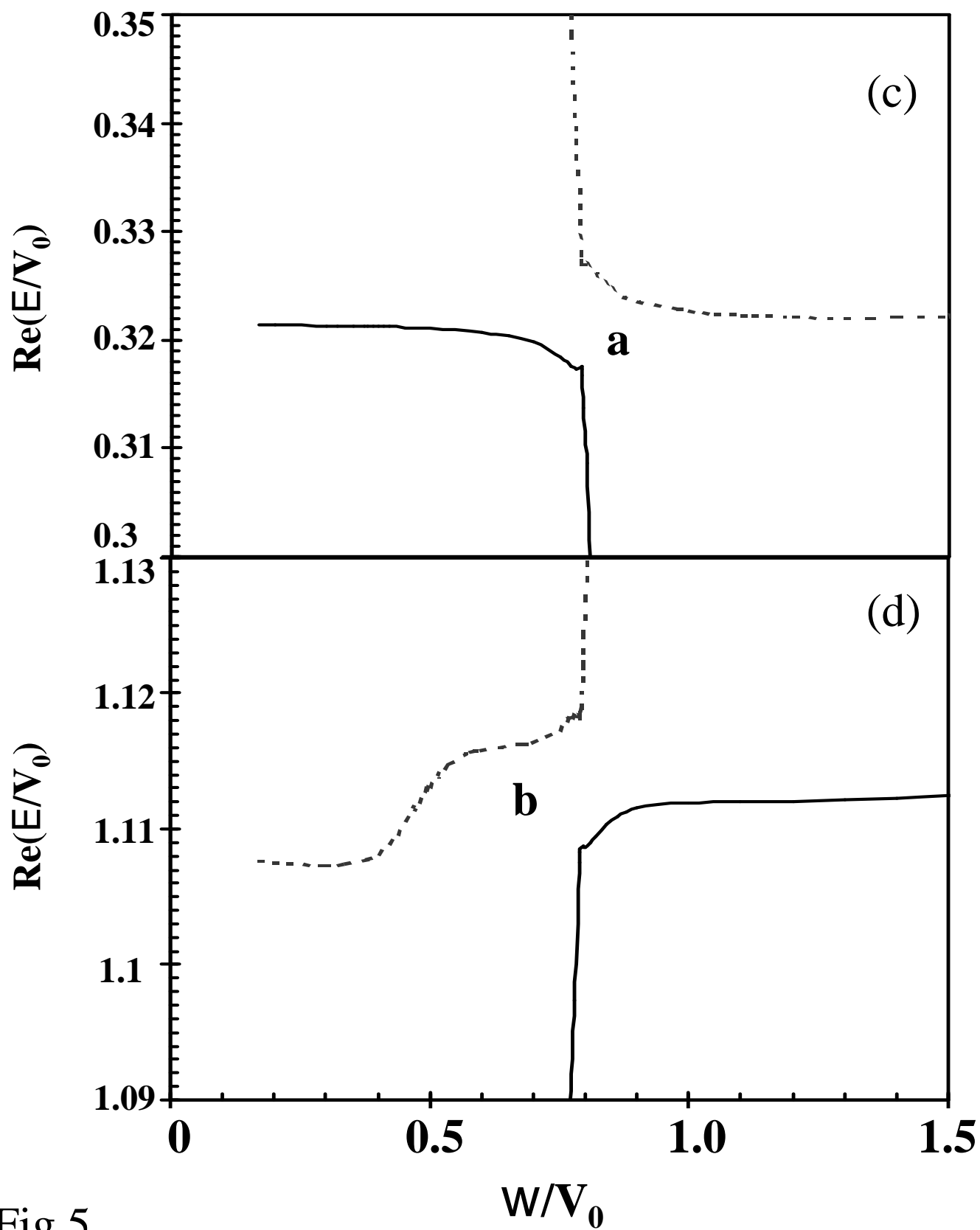


Fig.5

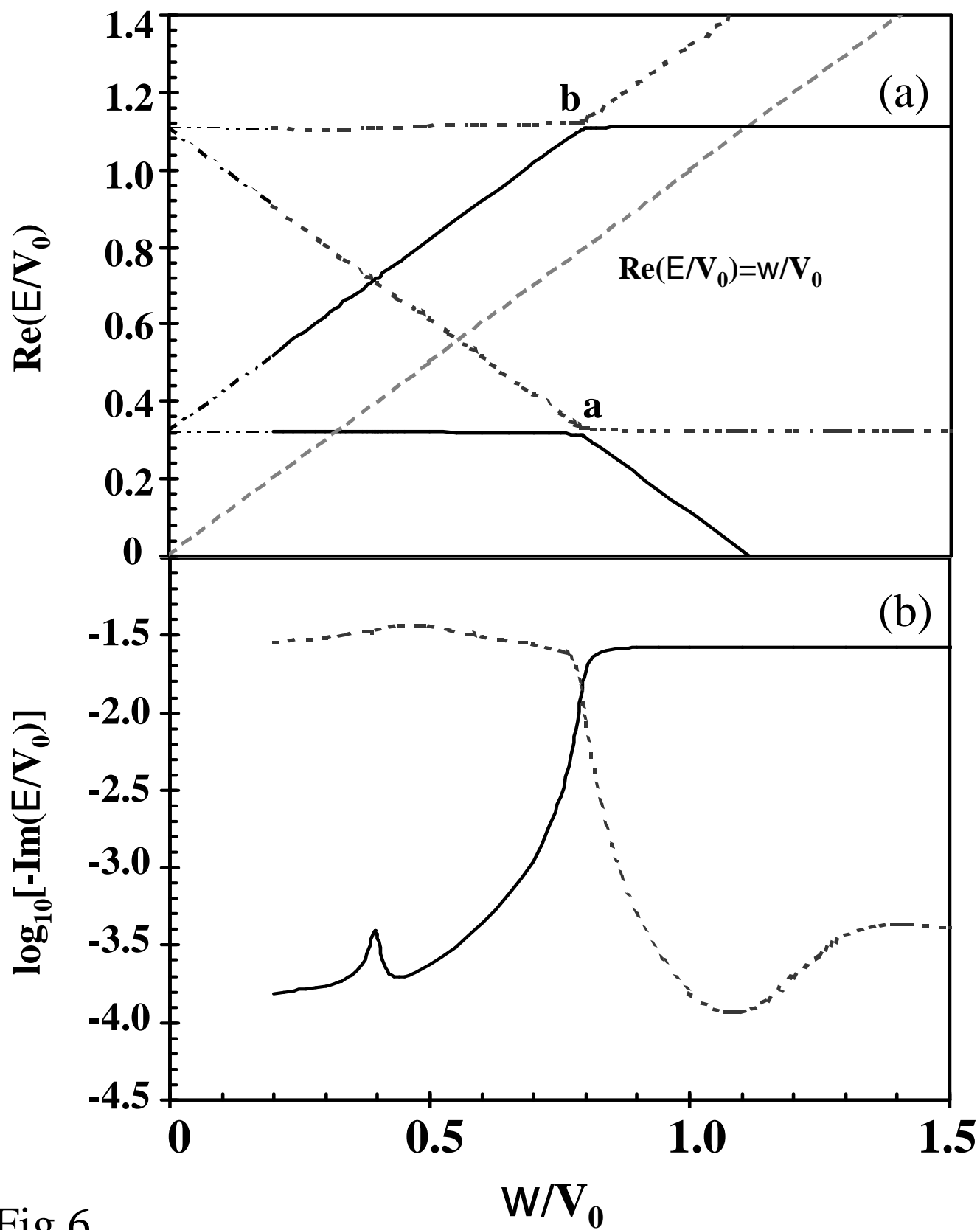


Fig.6

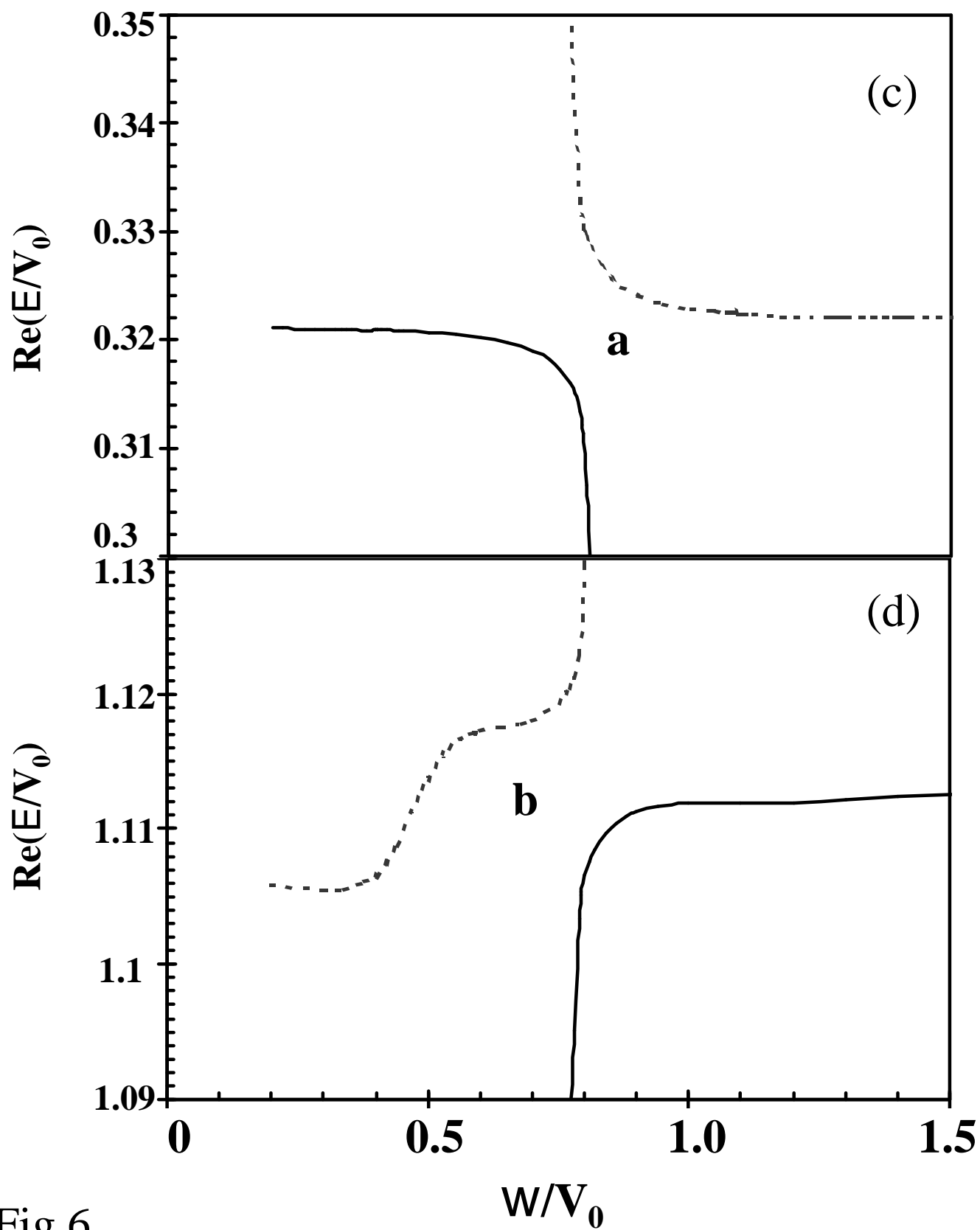


Fig.6

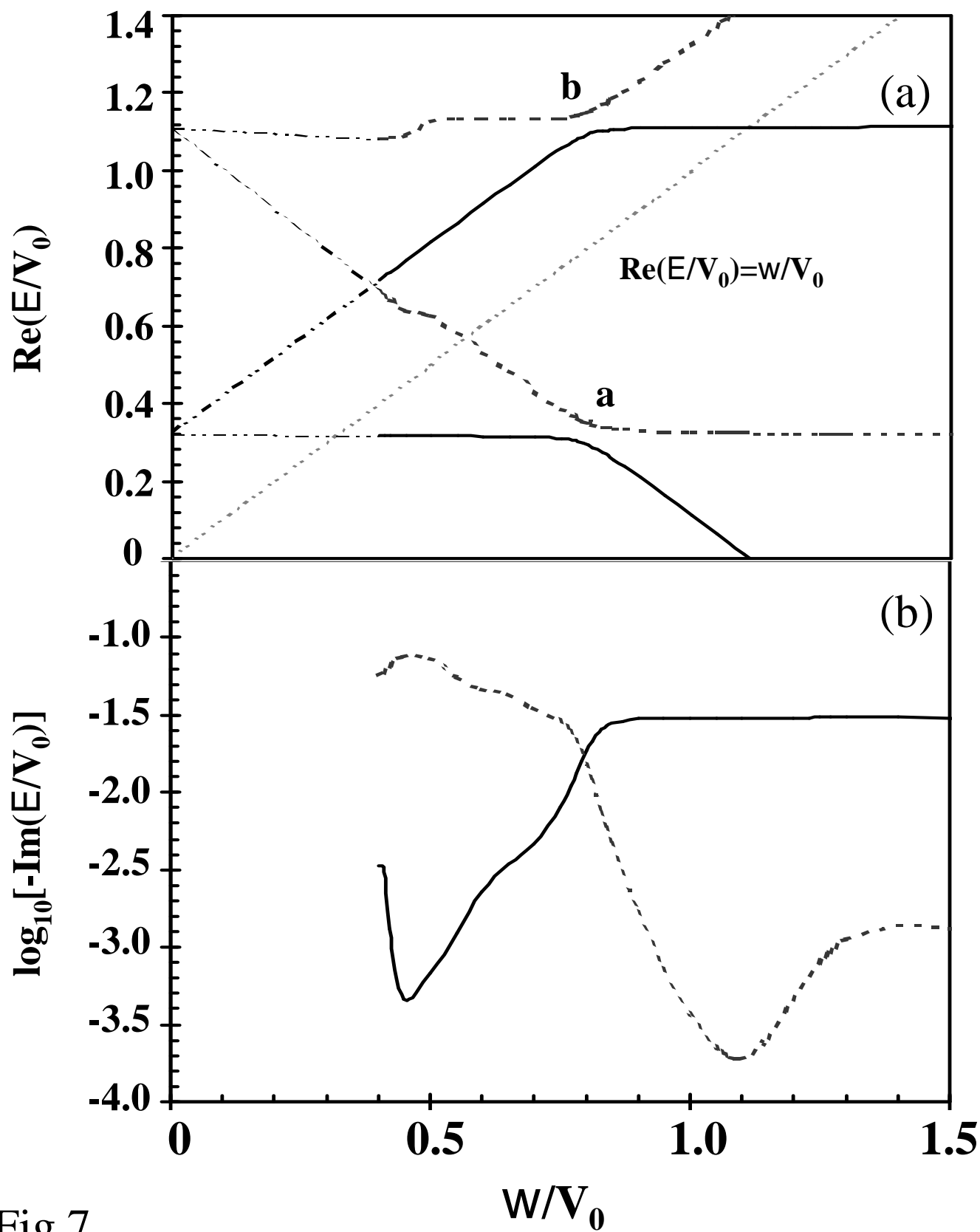


Fig.7

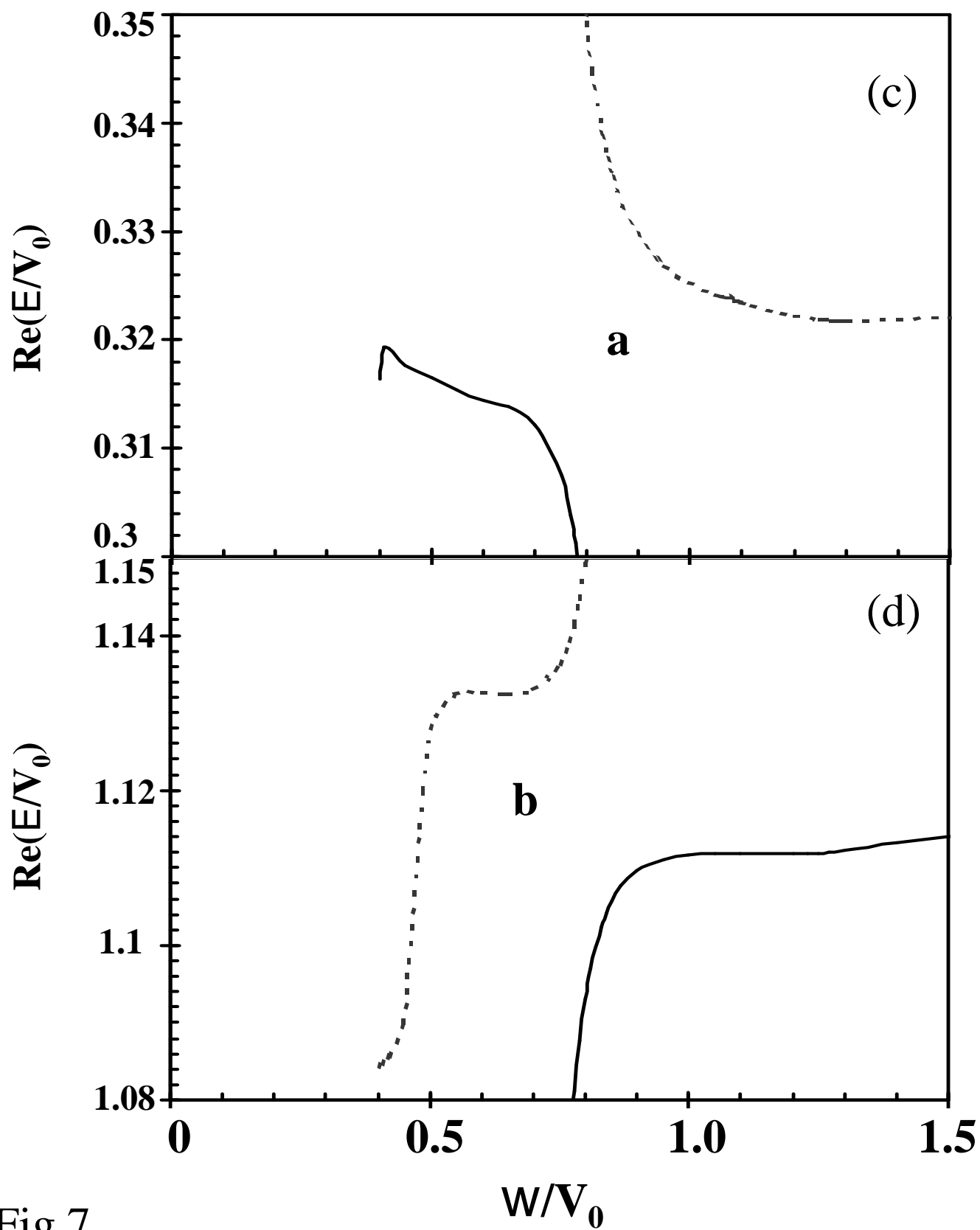


Fig.7